

Detailed analysis of shake structures in the *KLL* Auger spectrum of H₂SR. Püttner,¹ D. Céolin,² R. Guillemin,³ R. K. Kushawaha,³ T. Marchenko,³ L. Journel,³ M. N. Piancastelli,^{3,4} and M. Simon^{2,3}¹*Institut für Experimentalphysik, Freie Universität Berlin, D-14195 Berlin, Germany*²*Synchrotron SOLEIL, l'Orme des Merisiers, Saint-Aubin, FR-91192 Gif-sur-Yvette Cedex, France*³*Sorbonne Universités, UPMC Univ Paris 06, CNRS, UMR 7614, Laboratoire de Chimie Physique-Matière et Rayonnement, F-75005 Paris, France*⁴*Department of Physics and Astronomy, Uppsala University, SE-75120 Uppsala, Sweden*

(Received 12 December 2015; published 4 April 2016)

Shake processes of different origin are identified in the *KLL* Auger spectrum of H₂S with unprecedented detail. The *KLL* Auger spectrum is presented together with the S 1s⁻¹ photoelectron spectrum including the S 1s⁻¹V⁻¹nλ and S 1s⁻¹2p⁻¹nλ shake-up satellites with V⁻¹ and nλ indicating a hole in the valence shell and an unoccupied molecular orbital, respectively. By using different photon energies between 2476 and 4150 eV to record the *KLL* Auger spectra two different shake-up processes responsible for the satellite lines are identified. The first process is a shake-up during the Auger decay of the S 1s⁻¹ core hole and can be described by S 1s⁻¹ → 2p⁻²V⁻¹nλ. The second process is the Auger decay of the shake-up satellite in the ionization process leading to S 1s⁻¹V⁻¹nλ → 2p⁻²V⁻¹nλ transitions. By combining the results of photoelectron and Auger spectra the involved V⁻¹nλ levels are assigned.

DOI: [10.1103/PhysRevA.93.042501](https://doi.org/10.1103/PhysRevA.93.042501)

I. INTRODUCTION

The *KLL* Auger spectra of third-row elements are highly complex, including the so-called diagram lines as well as different types of shake structures. While the diagram lines are readily identified, a detailed assignment of all types of shake features has not yet been reported in an atomic or molecular case, due to the presence of multiple structures and the fact that a suitable method to distinguish between them has not yet been developed. In the present work, we demonstrate that, using a synchrotron light source with its ability to provide photons of tunable energy, the different Auger processes can readily be distinguished by the lowest photon energy at which they appear in the Auger spectrum. Therefore a complete assignment of the *KLL* Auger spectrum is provided in a prototypical molecular system, H₂S, including all types of shake processes possible during the relaxation of a deep core hole.

The *KLL* Auger spectra of argon [1–3] as well as of molecules with other third-row elements [3–5] have been studied extensively in the 1970s. The spectra are dominated by the so-called diagram lines, i.e., the atomic-like 1s⁻¹ → 2s⁻²(¹S₀), 1s⁻¹ → 2s⁻¹2p⁻¹(¹P₁, ³P_{0,1,2}), and 1s⁻¹ → 2p⁻²(¹S₁, ¹D₂, ³P_{0,2}) transitions. The energy positions of these transitions are mainly given by the decaying atom, with a minor but equal shift for all transitions caused by the chemical surrounding.

Contrary to this, in the shake satellites transitions from valence levels to unoccupied orbitals close to the ionization threshold are involved. Because of this the shake structures depend strongly on the detailed electronic structure of the molecule. The shake process can take place in both the photoionization and the decay process; in the following these two processes are labeled type II and type I, respectively; see Fig. 1. Moreover, in case of a shake during the photoionization process, one can further distinguish between shakes from the valence shell (type IIa) or from a core level (type IIb). In a more formal way, the entire ionization and decay process for

the production of these three types of satellite lines can be described as follows:

$$\text{type I : g.s.} \rightarrow 1s^{-1} \rightarrow 2(s,p)^{-2}V^{-1}n\lambda$$

$$\text{type IIa : g.s.} \rightarrow 1s^{-1}V^{-1}n\lambda \rightarrow 2(s,p)^{-2}V^{-1}n'\lambda$$

$$\text{type IIb : g.s.} \rightarrow 1s^{-1}2(s,p)^{-1}n\lambda \rightarrow 2(s,p)^{-3}n'\lambda$$

Here g.s. and V⁻¹ describe the ground state and a vacancy in the valence shell, respectively, while nλ and n'λ denote unoccupied molecular orbitals including Rydberg orbitals or a continuum state; using n and n' as the principal quantum number allows accounting for the possibility of a shake process in each step, the photoionization, and the Auger decay.

Up to now, the shake structures in the *KLL* spectra of third-row elements were explained with the Auger decays of the type II, i.e., shake satellites produced during the photoionization process. In particular, the *KLL* Auger satellites of H₂S have been discussed by Faegri and Keski-Rahkonen in terms of processes of type IIb [4] and by Asplund *et al.* mainly in terms of processes of type IIa [5].

In the *KLL* Auger spectra of the molecules HCl, PH₃, and SiH₄ satellite lines were observed but not assigned to a specific process [3]. For argon the satellites are explained with processes of the type IIa and IIb [2]. In case of neon [6] the satellites are explained with *KL* → *LLL* transitions, which can be assigned to both the processes of the type IIa and IIb, due to the fact that the *L* shell is identical to the valence shell. In all these analyses the shake processes of type I, i.e., a shake during the Auger decay, are fully neglected in the explanation of *KLL* Auger spectra, although they are very common in the resonant Auger decay [7–10], i.e., when one electron is in an open orbital close to the ionization threshold. The last statement is in line with the fact that in nonresonant *KLL* Auger spectra the satellites of type I have only been reported for the open-shell atom sodium [11]. In addition, a discrepancy between experiment and theory of the open-shell atom silicon is also referred to Auger processes of type I [12].

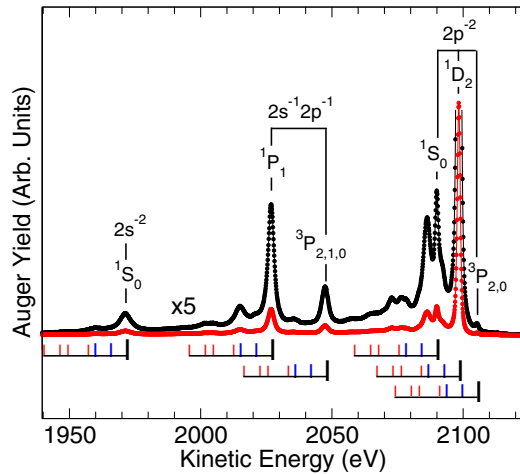


FIG. 3. Overview spectrum of the *KLL* Auger transitions in H_2S measured subsequent to a photoionization with 4150 eV photons. The diagram lines are indicated with vertical-bar diagrams above the spectrum. The vertical bar diagrams below the spectrum indicate the energy positions of the identified lines. For each bar diagram the large black, medium blue, and small red bars indicate the energy position of the diagram line, shake satellites of type IIa (next two lines from the diagram line), and I (last 4 lines left of the diagram line), respectively. The Auger yield is given in arbitrary units by using a linear scale. For more details, see text.

record the $S\ 1s^{-1}2p^{-1}$ satellites presented in Fig. 2(b), and 1500–3000 sec for the *KLL* Auger spectra presented in Figs. 3 to 5, with times increasing with the photon energy.

To obtain accurate energies for the photoelectron and Auger spectra, energy calibration was achieved in two steps. First, the kinetic-energy scale of the electron analyzer was calibrated by measuring Ar *KMM* and *LMM* Auger spectra. The Auger energies were calculated from binding energies of 3206.3(3) eV [20], 248.63(1) eV [21,22], and 45.14(1) eV [23] for the $1s^{-1}$, $2p_{3/2}^{-1}$, and $3p^{-2}(^1D_2)$ states of argon, respectively. Second, the photon energy was calibrated by measuring Ar $1s^{-1}$ and $2p_{3/2}^{-1}$ photoelectron spectra using the previously calibrated kinetic-energy scale. Overall the binding energies for the double core-hole states were determined with a systematic uncertainty of 0.4 eV. The accuracy of the binding energies is limited mostly by uncertainty in the literature value of the $1s^{-1}$ binding energy of 0.3 eV. From the described energy calibration a kinetic energy of $E_{\text{kin}} = 2098.33(40)$ eV for the $1s^{-1} \rightarrow 2p^{-2}(^1D_2)$ Auger transition and a binding energy of $E_{\text{bin}} = 2478.25(40)$ eV for the $S\ 1s^{-1}$ ionization is obtained. These results agree within the error bars with the values $E_{\text{kin}} = 2098.51$ eV and $E_{\text{bin}} = 2478.32$ eV reported by Carroll *et al.* [24]. For the Auger spectra recorded over a wide kinetic energy range of 180 eV the transmission efficiency of the detector is estimated to be constant within 3%, with a tendency to drop towards higher kinetic energies.

III. RESULTS AND DISCUSSION

A. The $S\ 1s^{-1}$ photoelectron spectrum

As mentioned above, the different processes causing *KLL* Auger satellites can be distinguished by the photon energy used

for the ionization. In order to identify possible initial states of the satellite decays and to find well-suited photon energies to measure the Auger spectra, the $S\ 1s^{-1}$ photoelectron spectrum including the $S\ 1s^{-1}V^{-1}n\lambda$ and $S\ 1s^{-1}2p^{-1}n\lambda$ shake-up satellites are measured and displayed in Fig. 2. The $1s^{-1}2p^{-1}$ double core-hole states have been reported in literature up to now only for the atomic system of argon, showing that their intensities are in the order of less than 5×10^{-4} of the Ar $1s^{-1}$ main line [25]. The observation of satellite structures with such low intensities is possible only with a state-of-the-art experimental setup like the present high-resolution electron analyzer equipped with a gas cell in combination with a beam line that provides high photon flux [16,17]. The $S\ 1s^{-1}2s^{-1}n\lambda$ satellites are not recorded. However, based on the results for double core-hole shake-up satellites of argon, they are expected to be approximately one order of magnitude weaker than the $S\ 1s^{-1}2p^{-1}n\lambda$ satellites [25] so they do not play a role in the present study; see below.

A detailed analysis of the $S\ 1s^{-1}2p^{-1}n\lambda$ shake-up spectrum is beyond the scope of the publication and will be presented elsewhere [26]. However, the $S\ 1s^{-1}V^{-1}n\lambda$ shake-up spectrum of H_2S contains important information for the present study, so an approach to the assignment will be given here. In Fig. 2 seven peaks are indicated. The structure formed by peaks 3 to 7 looks rather similar to the $O\ 1s^{-1}V^{-1}n\lambda$ shake-up spectrum of H_2O [27], which has a similar valence structure. The latter spectrum was assigned by Sankari *et al.* by using symmetry-adapted cluster-configuration interaction (SAC-CI) calculations. Here we assign peaks 3 to 7 in the shake-up spectrum on the basis of these calculations for water and by taking into account the additional core-level shell of sulfur. In this way we assign peak 3 to the $S\ 1s^{-1}5a_1^{-1}6a_1$ excitation and peak 4 to $S\ 1s^{-1}2b_2^{-1}3b_2$ mixing partially with $S\ 1s^{-1}2b_2^{-1}4pb_2$. For the narrow peak 5 visible 15.4 eV above the main line we obtain an assignment to a state with the dominant configurations $S\ 1s^{-1}2b_2^{-1}4pb_2$ plus $S\ 1s^{-1}2b_1^{-1}4pb_1$. The broader peak 6 present 18.4 eV above the main line thus consists of three states with the dominant configurations $S\ 1s^{-1}5a_1^{-1}4sa_1$ plus $S\ 1s^{-1}5a_1^{-1}4pa_1$, $S\ 1s^{-1}2b_1^{-1}4pb_1$ plus $S\ 1s^{-1}2b_1^{-1}5pb_1$, and $S\ 1s^{-1}2b_1^{-1}5pb_1$. Finally, peak 7 shows shake transitions to higher- n Rydberg states. The present approach clearly suggests that the shake-up predominantly leads to an occupation of low- n Rydberg states, but not of the unoccupied valence orbitals $6a_1$ and $3b_2$.

Peaks 1 and 2 approximately 6 and 10 eV above the $S\ 1s^{-1}$ main line are considered to be too low for being caused by shake satellites. However, their energy position agrees well with the main lines in the valence shell photoabsorption spectrum of H_2S [28] suggesting an energy loss of the $S\ 1s^{-1}$ main line electrons caused by inelastic scattering from H_2S molecules in the gas target. Such an assignment has already been suggested by Southworth *et al.* for the Ar $1s^{-1}$ photoelectron spectrum [29]. The peaks for argon assigned by Southworth *et al.* to inelastic scattering have been reproduced in the present studies by using pressure conditions comparable to those for present H_2S measurements.

TABLE I. Kinetic energy E_{kin} and assignment of the diagram and satellite lines observed in *KLL* Auger spectrum of H_2S . The energy positions of the diagram lines are given in absolute values while the energy positions for the satellite lines are relative to the main lines. The first two satellites below the diagram line are of type IIa, and the remaining correspond to type I. All errors are given in parentheses and apply to the last digit(s). All absolute values are additionally subject to an error of 0.4 eV due to calibration of the energy scale, which has not been included in the error bars.

E_{kin} (eV)	Assignment
<i>Diagram lines</i>	
2106.31(4)	$1s^{-1} \rightarrow 2p^{-2}(^3P_2)$
2098.33(1)	$1s^{-1} \rightarrow 2p^{-2}(^1D_2)$
2090.99(3)	$1s^{-1} \rightarrow 2p^{-2}(^1S_0)$
2047.39(10)	$1s^{-1} \rightarrow 2s^{-1}2p^{-1}(^3P_{2,1,0})$
2026.83(10)	$1s^{-1} \rightarrow 2s^{-1}2p^{-1}(^1P_1)$
1971.25(10)	$1s^{-1} \rightarrow 2s^{-2}(^1S_0)$
<i>Satellite lines</i>	
-6.0(5)	$1s^{-1} \text{ low-}n \text{ Ryd} \rightarrow 2(s,p)^{-2} \text{ low-}n \text{ Ryd}$
-12.0(2)	$1s^{-1} \text{ low-}n \text{ Ryd} \rightarrow 2(s,p)^{-2} \text{ higher-}n \text{ Ryd}$
-14.6(2)	$1s^{-1} \rightarrow 2(s,p)^{-2}5a_1^{-1}6a_1$ or $1s^{-1} \rightarrow 2(s,p)^{-2}2b_1^{-1}2b_1$
-22.3(2)	$1s^{-1} \rightarrow 2(s,p)^{-2}V^{-1} \text{ low-}n \text{ Ryd}$
-25.4(2)	$1s^{-1} \rightarrow 2(s,p)^{-2}V^{-1} \text{ low-}n \text{ Ryd}$
-31.5(3)	$1s^{-1} \rightarrow 2(s,p)^{-2}V^{-1} \text{ higher-}n \text{ Ryd}$

B. The *KLL* Auger spectrum

Figure 3 shows the *KLL* Auger spectrum of H_2S subsequent to a S $1s$ ionization using 4150 eV photons. The diagram lines $2s^{-2}(^1S_0)$, $2s^{-1}2p^{-1}(^1P_1, ^3P_{2,1,0})$, $2p^{-2}(^1S_0, ^1D_2, ^3P_{2,0})$ were already clearly assigned in previous studies [4,5] based on theoretical results. Note that the Auger transition to the $2p^{-2}(^3P)$ final state is forbidden in *LS* coupling by angular momentum and parity conservation. The $1s^{-1} \rightarrow 2p^{-2}(^3P_{2,0})$ transitions obtain some intensity by mixing with the final states $2p^{-2}(^1S_0, ^1D_2)$ via spin-orbit interaction, while the $1s^{-1} \rightarrow 2p^{-2}(^3P_1)$ Auger transition remains absent due to the absence of a mixing partner with $J = 1$ [30]. In addition to the diagram lines, a large number of satellite lines can be observed. The satellite lines are indicated in Fig. 3 by the vertical-bar diagrams below the spectrum, and their energy positions as well as their assignments are given in Table I, together with the energy positions of the diagram lines. As mentioned above, these satellites have been discussed by Faegri and Keski-Rahkonen in terms of processes of type IIb [4] and by Asplund *et al.* mainly in terms of processes of type IIa [5].

Figure 4 shows the *KLL* Auger spectrum recorded subsequent to photoionization with different photon energies between 2476 and 2495 eV. The S $1s$ threshold is located at 2478.25 eV so that the spectra below this value are dominated by resonant Auger transitions. For all spectra, the Auger yield axis is expanded in order to focus on the relatively weak satellite lines. The black, blue, and red vertical dashed lines indicate the energy position of the $2s^{-2}(^1S_0)$, $2s^{-1}2p^{-1}(^1P_1)$, and $2p^{-2}(^1D_2)$ diagram lines. The $2s^{-2}(^1S_0)$ diagram line shifts from 2495 to 2479 eV by 1.08 eV to higher kinetic energies due to postcollision interaction (PCI). This value is in good agreement with the PCI shift for the Ar $1s \rightarrow 2p^{-2}(^1D_2)$ Auger

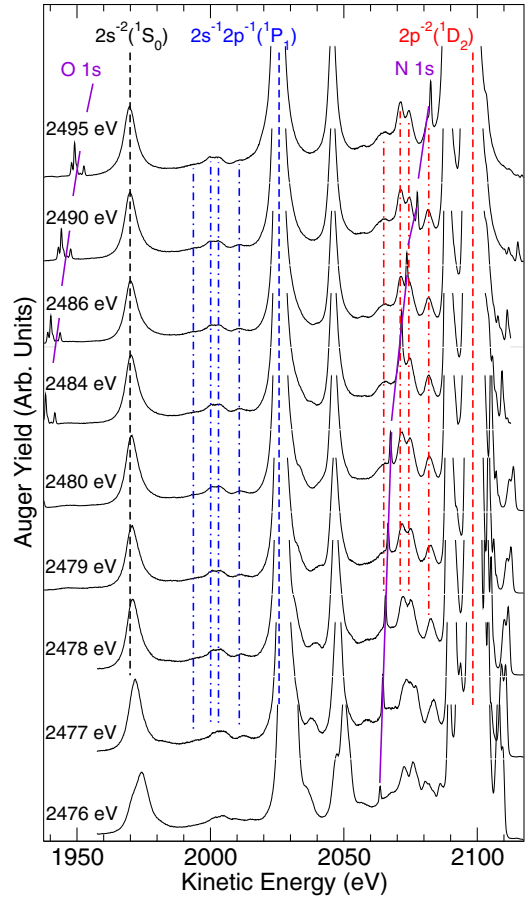


FIG. 4. The *KLL* Auger spectrum measured subsequent to photoionization with different photon energies between 2476 and 2495 eV and a focus on low intensities. The black, blue, and red vertical dashed lines indicate the energy position of the $2s^{-2}(^1S_0)$, $2s^{-1}2p^{-1}(^1P_1)$, and $2p^{-2}(^1D_2)$ diagram lines. The colored dash-dotted lines indicate energy positions of satellite lines associated with the diagram line indicated with the same color. The diagonal violet lines indicate impurities caused by photoelectron spectra of nitrogen- and oxygen-containing molecules. The photoelectron yields are given in arbitrary units by using a linear scale.

transition observed close to threshold [31,32]. A similar shift can also be seen for the $2s^{-1}2p^{-1}(^1P_1)$, and $2p^{-2}(^1D_0)$ diagram lines, indicated by the blue and red dashed lines, respectively.

The vertical dash-dotted lines indicate satellite Auger transitions which show up directly at the S $1s$ photoionization threshold of 2478.25 eV. Below this value they are also visible, however, shifted to higher kinetic energies as expected for resonant Auger lines. This behavior clearly shows that the discussed satellite lines are due to shake processes occurring during the Auger decay, i.e., they are processes of type I. As discussed above, such Auger satellites have been observed to our knowledge only for open-shell atoms but not for molecules.

The kinetic energies of the Auger satellites indicated with blue and red dash-dotted lines are by 14.6, 22.3, 25.4, and 31.5 eV below those of the $2s^{-1}2p^{-1}(^1P_1)$ and $2p^{-2}(^1D_2)$ diagram lines, respectively. These constant splittings relative to the diagram lines suggest to assign the satellites as transitions to the final states $2s^{-1}2p^{-1}(^1P_1)$ and $2p^{-2}(^1D_2)$ accompanied

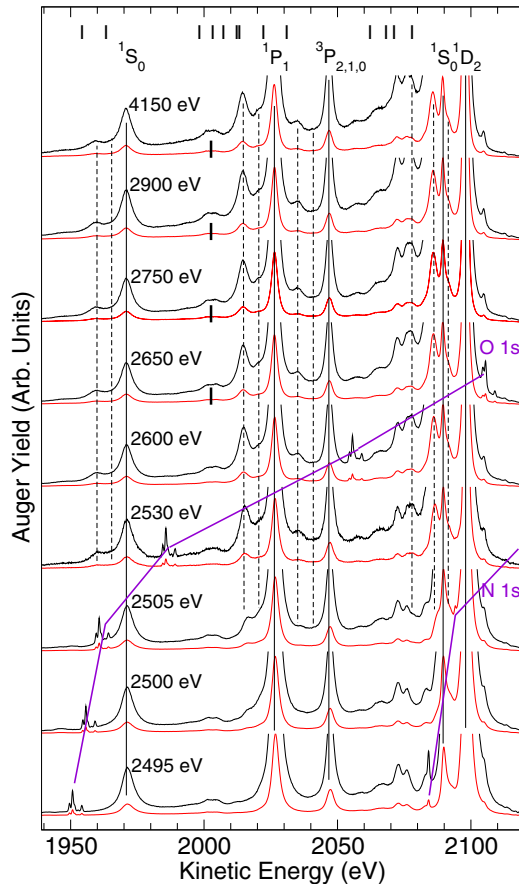


FIG. 5. The *KLL* Auger spectrum measured subsequent to photoionization with different photon energies between 2495 and 4150 eV and a focus on low intensities. For the black curves the intensity is multiplied by a factor of four relative to the red curves. The solid vertical lines indicate the diagram lines and the dashed vertical lines satellite transitions of the type IIa. The solid bars in the spectra measured with photon energies of 2650 eV and above indicate identical relative intensities at 2003 eV. The solid bars above the spectra show the theoretical energy positions of the $KL_{2,3} \rightarrow LLL_{2,3}$ Auger transitions, of type IIb, taken from Ref. [4]. The diagonal violet lines indicate impurities caused by photoelectron spectra of nitrogen- and oxygen- containing molecules. The Auger yields are given in arbitrary units by using a linear scale. For more details, see text.

with a shake process in the valence shell. In addition to the discussed satellite lines, a weak line at $\cong 2058.0$ eV can be found. This value is $\cong 31.5$ eV below that of the $2p^{-2}(^1S_0)$ diagram line so that the line at $\cong 2058.0$ eV can be related to the latter diagram line. The assignment of the lines will be given further below.

We expect that such satellites belonging to the other diagram lines are also present in the spectrum. They have, however, much lower intensities, due to the intensities of the corresponding diagram lines, and they are expected at energies where they overlap with more intense lines so that they cannot be observed; see lower vertical bar diagrams in Fig. 3.

Figure 5 shows the Auger spectrum measured after photoionization with different photon energies between 2495 and 4150 eV. The diagram lines are indicated with solid vertical bars. The dashed lines indicate satellite Auger transitions

which are located $\cong 6$ and 12.0 eV below the corresponding diagram line. The more intense satellite visible 12.0 eV below the diagram line can be observed for the states $2s^{-2}(^1S_0)$, $2s^{-1}2p^{-1}(^1P_1)$, and $2p^{-2}(^1D_2)$. In contrast to this, the satellite $\cong 6$ eV below the diagram line is not observed for the state $2p^{-2}(^1S_0)$. The missing 6 eV satellite for the $2p^{-2}(^1S_0)$ state and both satellites for the states $2p^{-2}(^3P_{2,0})$ can readily be explained with their low intensity in combination with an overlap with other, more intense spectral features.

The two discussed satellites are visible only in the spectra measured at 2505 eV or above and develop their full intensity in the 2530 eV spectrum. This energy-dependent behavior suggests that these satellites are related to the normal Auger of $1s^{-1}V^{-1}n\lambda$ satellites in the photoelectron spectrum; i.e., they are due to processes of type IIa.

In the following we shall give an approach to the assignment of the satellite lines of type I and type IIa. As shown in Fig. 1, the final states of the type I satellite are energetically located 14.6, 22.3, 25.4, and 31.5 eV above the corresponding $S 2(s,p)^{-2}$ state. Interestingly, the less intense satellite transition of type IIa has a transition energy which is $\cong 6$ eV less than the transition energy of the diagram lines. By assuming that the less intense lines originate from the spectator Auger decay of the strongest satellites in the photoelectron spectrum, i.e., 15.4 and 18.5 eV above the $S 1s^{-1}$ state, one ends up in states $\cong 21.5$ and $\cong 24.5$ eV above the $S 2(s,p)^{-2}$ states. These energies agree well with the final states of the most intense satellite lines of type I, and the slight differences may be explained by the influence of the nuclear dynamics. By assigning these satellite lines of type IIa as $S 1s^{-1}V^{-1}n\lambda \rightarrow 2p^{-2}V^{-1}n'\lambda$ transitions with $n\lambda$ being low- n Rydberg states, i.e., to spectator Auger decays, we obtain a consistent assignment; see below. As a direct consequence the levels 22.3 and 25.4 eV above the $2p^{-2}$ states, which are the final states of the discussed Auger decays, are labeled as low- n Rydberg states. This assignment is in line with the assumption that for the shake satellites during the Auger decay the transitions to the low- n Rydberg states are the most intense ones, in analogy to the observation for the $S 1s^{-1}V^{-1}n\lambda$ shake-up satellites in the photoelectron spectrum. Based on this, the state 14.6 eV above the $2p^{-2}$ states can be assigned to $2p^{-2}5a_1^{-1}6a_1$ or $2p^{-2}2b_2^{-1}3b_2$ shake-up satellites, i.e., shake-up processes in the unoccupied valence orbitals. Such shake-up states have been calculated to be the lowest ones in the $O 1s^{-1}$ photoelectron spectrum of water, showing a rather low shake probability; see above. Finally, the state 31.5 eV above the $S 2(s,p)^{-2}$ state might be a higher- n Rydberg state. The given assignment for the states allows to attribute the stronger satellite transitions of type IIa, which are 12 eV below the corresponding diagram lines, to a $S 1s^{-1}V^{-1}n\lambda \rightarrow 2p^{-2}V^{-1}n'\lambda$ shake up transition, here $n\lambda$ being a low- n Rydberg state and $n'\lambda$ a higher- n Rydberg state.

The latter assignment becomes plausible by considering that the Rydberg states see in good approximation a H_2S^{3+} molecular core due to the two vacancies in the $2(s,p)$ shell as well as one vacancy in the valence shell. The energy position E of Rydberg states relative to the ionization threshold can be described by

$$E = -\frac{\text{Ry}Z^2}{(n-\delta)^2} \quad (1)$$

with Ry being the Rydberg constant, Z the charge seen by the Rydberg electron, n the principal quantum number of the Rydberg state, and δ the quantum defect. In the K -shell photoabsorption spectrum of H_2S , the two lowest Rydberg states $1s^{-1}4p$ and $1s^{-1}5p$ see a charge of $+1$ and are split by 1.1 eV [33]. Scaling this value with a factor of 9 due to the charge of $+3$ in the present case leads to a splitting of $\cong 10$ eV, which is in reasonable agreement with the present results. Nevertheless, all given assignments of the satellites have to be considered tentative and require additional theoretical confirmation, which is beyond the scope of the present work.

The S $1s^{-1}2p^{-1}$ satellites depicted in Fig. 2(b) suggest to take also the corresponding Auger decays, i.e., type IIb into account. These decays are expected in the spectra measured above 2700 eV. A careful comparison of the spectra below and above 2700 eV does not show additional spectral features that can be related to the Auger decay of S $1s^{-1}2p^{-1}$ shake satellites. However, in two regions, namely around 2000 and 2075 eV, an increase of the background can be observed. This can be seen, e.g., in the region around 2000 eV by the bold vertical bars indicating identical relative intensities. In the region around 2090 eV the $2p^{-2}(^1S_0)$ diagram line has identical relative intensity, while in the region around 2075 eV the intensity increases above 2700 eV photon energy. These changes in intensity are unclear but may be related to the Auger decay of the S $1s^{-1}2p^{-1}n\lambda$ shake satellites. For this purpose, the energy positions of the $KL_{2,3} \rightarrow LLL_{2,3}$ Auger transitions taken from Ref. [4] are indicated in the upper part of the figure. Interestingly, the calculated energy positions of the Auger decays to the $2p^{-3}$ final states around 2075 eV and $2s^{-1}2p^{-2}$ final states between 2000 and 2030 eV agree reasonably well with the energy regions with increasing background, suggesting a possible connection.

IV. SUMMARY AND CONCLUSIONS

In the present work, an approach is developed to allow identifying the shake processes of different nature occurring in the complex Auger decay after deep core excitation in the prototypical molecular system H_2S . To perform such detailed analysis, the finding is exploited that different shake processes appear at different distances from the photoionization threshold and therefore can be identified by varying the photon energy. Specifically, the KLL Auger spectrum is presented together with the S $1s^{-1}$ photoelectron spectrum including the

S $1s^{-1}V^{-1}n\lambda$ and S $1s^{-1}2p^{-1}n\lambda$ shake-up satellites. The S $1s^{-1}V^{-1}n\lambda$ satellites are preliminarily assigned by employing the similarity of the spectrum to that of H_2O [27], which has a isoelectronic valence shell. In the Auger spectrum six different satellite transitions are found. By varying the photon energy four of these lines were assigned to shake-up transitions during the Auger decay, i.e., S $1s^{-1} \rightarrow 2p^{-2}V^{-1}n\lambda$. The four resulting $2p^{-2}V^{-1}n\lambda$ final states are 14.6 , 22.3 , 25.4 , and 31.5 eV above the corresponding $2p^{-2}$ state.

Two more Auger satellites are due to the Auger decay of the satellite lines in the photoelectron spectrum. They can be described as S $1s^{-1}V^{-1}n\lambda \rightarrow 2p^{-2}V^{-1}n'\lambda$ with $n \leq n'$; here $n = n'$ stays for a spectator Auger decay and $n < n'$ for a second shake-up process of the already shaken electron. By combining the assignment of the S $1s^{-1}V^{-1}n\lambda$ shake-up structures of the photoelectron spectrum with the different satellite Auger lines, the tentative assignment $2p^{-2}5a_1^{-1}6a_1$ and/or $2p^{-2}2b_2^{-1}3b_2$ is given for the satellite state at 14.6 eV above the corresponding $2p^{-2}$ state, $2p^{-2}V^{-1}$ low- n Ryd for the states at 22.3 and 25.4 eV, and $2p^{-2}V^{-1}$ higher- n Ryd for the state at 31.5 eV. However, this assignment requires additional theoretical support.

The second type of satellite lines, the Auger decay of satellites in the photoelectron spectrum, is well known from previous studies. Contrary to this, the first type of satellites caused by shake-ups during the decay of the S $1s^{-1}$ core hole is observed for the first time in the KLL Auger spectrum of a closed-shell molecule. For the previously also suggested $KL_{2,3} \rightarrow LLL_{2,3}$ Auger transitions, no clear evidence is found.

Preliminary results on argon [34] are fully in line with the present findings, suggesting that both processes are also present in the KLL Auger spectra of other third-row elements like in HCl , PH_3 , SO_2 , SF_6 , or SiH_4 . Obviously similar studies for such molecules would shed light on the satellite structures, providing further information about the excited valence structure of molecules with double core-hole states.

ACKNOWLEDGMENTS

Experiments were performed on the GALAXIES beamline at SOLEIL Synchrotron, France (proposal number 20120642). We are grateful to the SOLEIL staff for the smooth operation of the facility.

-
- [1] M. O. Krause, Argon KLL Auger Spectrum: A Test of Theory, *Phys. Rev. Lett.* **34**, 633 (1975).
- [2] L. Asplund, P. Kelfve, B. Blomster, H. Siegbahn, and K. Siegbahn, Argon KLL and KLM Auger electron spectra, *Phys. Scr.* **16**, 268 (1977).
- [3] J. Vayrynen, R. N. Sodhi, and R. G. Cavell, Energies and intensities of the KLL Auger spectra of SiH_4 , PH_3 , HCl , and Ar, *J. Chem. Phys.* **79**, 5329 (1983).
- [4] K. Faegri and O. Keski-Rahkonen, Sulphur KLL Auger spectra of gaseous sulphur compounds, *J. Electron. Spectrosc. Relat. Phenom.* **11**, 275 (1976).
- [5] L. Asplund, P. Kelfve, B. Blomster, H. Siegbahn, K. Siegbahn, R. L. Lozes, and U. I. Wahlgren, Molecular Auger electron spectra of second row elements. Sulfur compounds, *Phys. Scr.* **16**, 273 (1977).
- [6] M. Leväsalmi, H. Aksela, and S. Aksela, Satellite structure in the KLL spectrum of neon, *Phys. Scr.* **T41**, 119 (1992).
- [7] P. A. Heimann, D. W. Lindle, T. A. Ferrett, S. H. Liu, L. J. Medhurst, M. N. Piancastelli, D. A. Shirley, U. Becker, H. G. Kerckhoff, B. Langer, D. Szostak, and R. Wehlitz, Shake-off on inner-shell resonances of Ar, Kr and Xe, *J. Phys. B* **20**, 5005 (1987).

- [8] H. Aksela, S. Aksela, H. Pulkkinen, G. M. Bancroft, and K. H. Tan, Anomalous strong shake-up processes in Auger decay of the resonantly excited $2p^5 3s^2 3p^6 nl$ states of Ar, *Phys. Rev. A* **37**, 1798(R) (1988).
- [9] S. Sundin, F. Kh. Gel'mukhanov, S. J. Osborne, O. Björneholm, A. Ausmees, A. Kikas, S. L. Sorensen, A. Naves de Brito, R. R. T. Marinho, S. Svensson, and H. Ågren, Auger decay of core-excited higher Rydberg states of carbon monoxide, *J. Phys. B* **30**, 4267 (1997).
- [10] R. Püttner, Y. F. Hu, G. M. Bancroft, A. Kivimäki, M. Jurvansuu, H. Aksela, and S. Aksela, Strong nonmonopole shake transitions in the Br $3d^{-1} np\pi$ ($n = 6-9$) resonant Auger spectra of HBr, *Phys. Rev. A* **77**, 032705 (2008).
- [11] T. Kantia, L. Partanen, S. Aksela, and H. Aksela, High resolution KLL Auger spectra of free sodium and magnesium atoms, *J. Electron Spectrosc. Relat. Phenom.* **180**, 58 (2010).
- [12] T. Kantia, S. Aksela, P. Turunen, L. Partanen, and H. Aksela, KLL Auger decay of atomic silicon, *J. Phys. B* **43**, 205002 (2010).
- [13] D. D. Sarma, C. Carbone, P. Sen, R. Cimino, and W. Gudat, Origin of Cu and Zn L_{2-} and $L_{3-}M_{45}M_{45}$ Auger Satellites: Breakdown of the Sudden Approximation, *Phys. Rev. Lett.* **63**, 656 (1989).
- [14] D. D. Sarma, C. Carbone, P. Sen, and W. Gudat, Synchrotron-radiation study of the satellites in Ni $L_{3-}M_{4,5}M_{4,5}$ Auger spectra, *Phys. Rev. B* **40**, 12542 (1989).
- [15] J. C. Woicik, P. Pianetta, S. L. Sorensen, and B. Crasemann, Photon-energy-sensitive Si $L_{2,3}VV$ Auger satellite, *Phys. Rev. B* **39**, 6048 (1989).
- [16] D. Céolin, J. M. Ablett, D. Prieur, T. Moreno, J.-P. Rueff, T. Marchenko, L. Journal, R. Guillemin, B. Pilette, T. Marin, and M. Simon, Hard x-ray photoelectron spectroscopy on the GALAXIES beamline at the SOLEIL synchrotron, *J. Electron Spectrosc. Relat. Phenom.* **190**, 188 (2013).
- [17] M. Simon, R. Püttner, T. Marchenko, R. Guillemin, R. K. Kushawaha, L. Journal, G. Goldsztejn, M. N. Piancastelli, J. M. Ablett, J.-P. Rueff, and D. Céolin, Atomic Auger doppler effects upon emission of fast photoelectrons, *Nat. Commun.* **5**, 4069 (2014).
- [18] M. O. Krause and J. H. Oliver, Natural widths of atomic K and L levels, K_{α} x-ray lines and several KLL Auger lines, *J. Phys. Chem. Ref. Data* **8**, 329 (1979).
- [19] M. Poygin, R. Püttner, M. Martins, V. Pennanen, M. Jurvansuu, Y. H. Jiang, H. Aksela, S. Aksela, and G. Kaindl, Detailed study of the $S2p^{-1} \rightarrow X^1A_1(2b_1^{-2})$ normal Auger spectra of H_2S , *Phys. Rev. A* **74**, 012711 (2006).
- [20] M. Breinig, M. H. Chen, G. E. Ice, F. Parente, B. Crasemann, and G. S. Brown, Atomic inner-shell level energies determined by absorption spectrometry with synchrotron radiation, *Phys. Rev. A* **22**, 520 (1980).
- [21] G. C. King, M. Tronc, F. H. Read, and R. C. Bradford, An investigation of the structure near the $L_{2,3}$ edges of argon, the $M_{4,5}$ edges of krypton and the $N_{4,5}$ edges of xenon, using electron impact with high resolution, *J. Phys. B* **10**, 2479 (1977).
- [22] L. Avaldi, G. Dawber, R. Camilloni, G. C. King, M. Roper, M. R. F. Siggel, G. Stefani, and M. Zitnik, Near-threshold photoionization of the Ar 2p subshell, *J. Phys. B* **27**, 3953 (1994).
- [23] NIST Atomic Level Database, Version 5, <http://www.nist.gov/pml/data/asd.cfm>.
- [24] T. X. Carroll, D. Ji, D. C. MacLaren, T. D. Thomas, and L. J. Saethre, Relativistic corrections to reported sulfur 1s ionization energies, *J. Electron Spectrosc. Relat. Phenom.* **42**, 281 (1987).
- [25] R. Püttner, G. Goldsztejn, D. Céolin, J.-P. Rueff, T. Moreno, R. K. Kushawaha, T. Marchenko, R. Guillemin, L. Journal, D. W. Lindle, M. N. Piancastelli, and M. Simon, Direct Observation of Double-Core-Hole Shake-Up States in Photoemission, *Phys. Rev. Lett.* **114**, 093001 (2015).
- [26] R. Püttner *et al.* (unpublished).
- [27] R. Sankari, M. Ehara, H. Nakatsuji, A. De Fanis, H. Aksela, S. L. Sorensen, M. N. Piancastelli, E. Kukkk, and K. Ueda, High resolution O 1s photoelectron shake-up satellite spectrum of H_2O , *Chem. Phys. Lett.* **422**, 51 (2006).
- [28] L. C. Lee, X. Wang, and M. Suto, Quantitative photoabsorption and fluorescence spectroscopy of H_2S and D_2S at 49–240 nm, *J. Chem. Phys.* **86**, 4353 (1987).
- [29] S. H. Southworth, T. LeBrun, Y. Azuma, and K. G. Dyall, Argon KM photoelectron satellites, *J. Electron. Spectrosc. Relat. Phenom.* **94**, 33 (1998).
- [30] V. Schmidt, *Electron Spectrometry of Atoms Using Synchrotron Radiation* (Cambridge University Press, Cambridge, 2005).
- [31] R. Huster, W. Sandner, and W. Mehlhorn, Post-collision interaction in inner-shell ionisation by electron impact: Energy shift of KLL Auger electrons of Ne and Ar, *J. Phys. B* **20**, L287 (1986).
- [32] R. Guillemin, S. Sheinerman, R. Püttner, T. Marchenko, G. Goldsztejn, L. Journal, R. K. Kushawaha, D. Céolin, M. N. Piancastelli, and M. Simon, Postcollision interaction effects in KLL Auger spectra following argon 1s photoionization, *Phys. Rev. A* **92**, 012503 (2015).
- [33] S. Bodeur and J. M. Esteva, Photoabsorption spectra of H_2S , CH_3SH and SO_2 near the sulfur K edge, *Chem. Phys.* **100**, 415 (1985).
- [34] R. Püttner *et al.* (unpublished).